

Approximate graphical method of solving Fermi level and majority carrier density of semiconductors with multiple donors and multiple acceptors

This article has been downloaded from IOPscience. Please scroll down to see the full text article.

2011 J. Semicond. 32 062001

(<http://iopscience.iop.org/1674-4926/32/6/062001>)

View [the table of contents for this issue](#), or go to the [journal homepage](#) for more

Download details:

IP Address: 130.199.3.165

The article was downloaded on 09/07/2013 at 17:58

Please note that [terms and conditions apply](#).

Approximate graphical method of solving Fermi level and majority carrier density of semiconductors with multiple donors and multiple acceptors

Ken K. Chin[†]

Department of Physics and Apollo CdTe Solar Energy Research Center, New Jersey Institute of Technology, Newark, NJ 07058, USA

Abstract: We present a generic approximate graphical method for determining the equilibrium Fermi level and majority carrier density of a semiconductor with multiple donors and multiple acceptors compensating each other. Simple and easy-to-follow procedures of the graphical method are described. By graphically plotting two wrapping step functions facing each other, one for the positive hole-ionized donor and one for the negative electron-ionized acceptor, we have the crossing point that renders the Fermi level and majority carrier density. Using the graphical method, new equations are derived, such as the carrier compensation proportional to N_A/N_D , not the widely quoted $N_A - N_D$. Visual insight is offered to view not only the result of graphic determination of Fermi level and majority carrier density but also the dominant and critical pair of donors and acceptors in compensation. The graphical method presented in this work will help to guide the design, adjustment, and improvement of the multiply doped semiconductors. Comparison of this approximate graphical method with previous work on compensation, and with some experimental results, is made. Future work in the field is proposed.

Key words: doping; compensation; Fermi level; carrier density; graphical method; ionization

DOI: 10.1088/1674-4926/32/6/062001

EEACC: 2520

1. Introduction

Localized impurity/defect electronic states in the bandgap of semiconductors are usually classified as dopants and deep levels^[1–3]. Those with an ionization or activation energy level less than 0.05 eV from the band edge are (shallow) dopants, and those with greater than 0.05 eV are deep levels^[2]. The dopants dope the semiconductor, determining its type (n or p), Fermi level, and carrier density. The deep levels may compensate the dopants but are mostly treated as generation-recombination centers, with a negative impact on the performance of most devices. Such a classification and description of the midgap states in a semiconductor is appropriate for the most widely used semiconductor materials, such as Si and GaAs, which usually have a single dominant dopant state of shallow energy level, typically ≤ 0.05 eV from the band edge^[1,2]. The concentration of the dominant shallow dopant is usually at least one order higher than that of the other dopants^[2] and many orders higher than that of the deep levels. Therefore, the majority carrier density of such a traditional non-degenerate semiconductor can be approximated by

$$n = N_C \exp \frac{E_F - E_C}{kT} \approx N_D - N_A \approx N_D, \quad (1)$$

$$p = N_V \exp \frac{E_V - E_F}{kT} \approx N_A - N_D \approx N_A, \quad (2)$$

where n , p , N_C , N_V , N_D , N_A , E_C , E_V , and E_F are electron density, hole density, the effective density of states in conduction band, the effective density of states in valence band, the shallow donor concentration, the shallow acceptor concentration,

the conduction band minimum (CBM), the valence band maximum (VBM), and the Fermi level, respectively. It is assumed that all donors and acceptors are ionized at room temperature, with

$$kT = 0.0259 \text{ eV}. \quad (3)$$

The usage and importance of non-traditional semiconductor materials, such as semi insulating semiconductors^[4], wide bandgap semiconductors^[5,6], transparent conducting oxides (TCO)^[7,8], as well as n-CdS and p-CdTe polycrystalline thin films used in solar cells^[9–12], have been steadily increasing. Due to either technical difficulties or cost considerations, the non-traditional, or rather the general semiconductor, may not have a clear demarcation to distinguish between shallow dopants and deep levels. Impurity and defect states, either donors or acceptors, of various atomic configuration and activation energy and of comparable concentration may all co-exist. Donors' doping and acceptors' compensation or anti-doping (or vice versa) may co-exist, with comparable concentrations, leading to the majority carrier density or even the type (n or p) of the semiconductor uncertain, vulnerable to unexpected dramatic change caused by some unknown or seemingly unimportant variations in condition in the processing of the material. For such non-traditional semiconductors, in determining its type, Fermi level, and majority carrier density due to compensation, instead of Eqs. (1) and (2), we need to resort to a general equation of the condition of local charge neutrality (LCN), valid for a semiconductor under equilibrium,

$$N_V \exp \frac{E_V - E_F}{kT} + \sum_i N_{D_i} \frac{1}{1 + g_D \exp \frac{E_F - E_{D_i}}{kT}}$$

[†] Corresponding author. Email: CHIN@NJIT.EDU
Received 22 December 2010

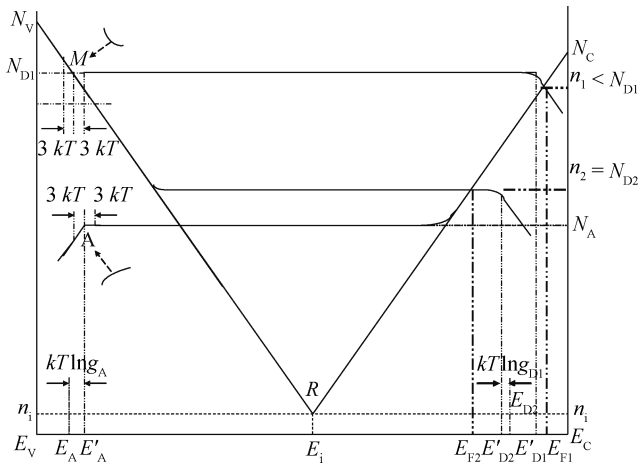


Fig. 1. Graphic representation of electrons, holes, donor states D₁ and D₂, and acceptor state A.

$$= N_C \exp \frac{E_F - E_C}{kT} + \sum_j N_{A_j} \frac{1}{1 + g_A \exp \frac{E_{A_j} - E_F}{kT}}, \quad (4)$$

where the left side is the positively charged hole and ionized donor densities, and the right side is the negatively charged electron and ionized acceptor densities. g_D and g_A are the degeneracy of the donor and acceptor states, respectively^[1,2,13]. For widely used tetrahedral cubic semiconductors, such as Si, GaAs, and CdTe, $g_D = 2$ due to spin degeneracy, and $g_A = 4$; in addition to spin degeneracy, the acceptor has the heavy hole and light hole degeneracy. With the energy level E_{D_i} and concentration N_{D_i} of all the i th donor states and the energy level E_{A_j} and concentration N_{A_j} of all the j th acceptor states given, we can solve Eq. (4) for the semiconductor's Fermi level E_F , from which we obtain the majority carrier density. For multiply doped materials, to do so analytically is impossible, and to do so numerically tends to lose the insight of the physical conditions of the system, such as which states are crucial and negligible in determining the Fermi level and majority carrier concentration. In this work, we present a simple approximate graphical method for the estimation of the results of compensation, or approximate solution of Eq. (4). To focus on the graphical method in this work, double donors, double acceptors and amorphetic deep levels will be discussed elsewhere.

2. Graphical representation of electrons, holes, donor states, and acceptor states

To solve Eq. (4) graphically, we use semi-logarithmic graph paper, with the energy levels E as x in linear scale, and the concentrations N as y in logarithmic scale. The first terms of the left and the right hand sides, representing the hole and electron density of non-degenerate semiconductor, are straight lines $N_V R$ of slope $-1/kT$ and $N_C R$ of slope $1/kT$, respectively, R indicates the intrinsic Fermi level E_i and intrinsic carrier density n_i ^[13]. Each dopant level is represented by a point D_i (for the i th donor) or A_j (for the j th acceptor) on the graph paper. The x - and y -coordinates of D_i and A_j are (E'_{D_i}, N_{D_i}) and (E'_{A_j}, N_{A_j}) , respectively, with

$$\begin{cases} E'_{D_i} = E_{D_i} - kT \ln g_D, \\ E'_{A_j} = E_{A_j} + kT \ln g_A. \end{cases} \quad (5)$$

Thus, Equation (4) can be rid of the degeneracy factors g_D and g_A , and simplified as

$$\begin{aligned} N_V \exp \frac{E_V - E_F}{kT} + \sum_i N_{D_i} \frac{1}{1 + \exp \frac{E_F - E'_{D_i}}{kT}} \\ = N_C \exp \frac{E_F - E_C}{kT} + \sum_j N_{A_j} \frac{1}{1 + \exp \frac{E'_{A_j} - E_F}{kT}}. \end{aligned} \quad (6)$$

For example, we consider the level of ionization of an acceptor state A, which is graphically represented by a horizontal line (full ionization) and a straight line of slope $1/kT$ (partial ionization), as shown in Fig. 1. The crossing of the two straight lines at the acceptor state's representing point A is to be rounded at $\pm 3kT$, beyond which the level of ionization is approximated by the two straight lines, since

$$\frac{N_A^-}{N_A} = \frac{1}{1 + \exp \frac{E'_A - E_F}{kT}} \approx 1 - \exp \frac{E'_A - E_F}{kT} > 95\%, \quad E_F > E'_A + 3kT, \quad (7)$$

and

$$\frac{N_A^-}{N_A} = \frac{1}{1 + \exp \frac{E'_A - E_F}{kT}} \approx \exp -\frac{E'_A - E_F}{kT} < 5\%, \quad E_F < E'_A - 3kT. \quad (8)$$

Similar round-up at $\pm 3kT$ can be done for the representing point of the acceptor state D_i , as well as for the merging points M of $N_V R$ and $N_D N_D^+$, and of $N_C R$ and $N_A N_A^-$. Therefore, as shown in Fig. 1, the graphic plotting of Eq. (6) is composed of only 3 types of straight lines: horizontal, with slope $-1/k$, and with slope $1/k$, with their crossing points and merging points rounded up.

3. Graphical solution of Fermi level and majority carrier density of multiply doped semiconductors

To solve the equilibrium Fermi level and majority carrier density graphically of a semiconductor due to compensation of multiple dopants, we follow the following procedures:

- (1) Plot the representative points of two types of dopants D_i and A_j .
- (2) From each D_i and A_j , draw a step function composed of a horizontal straight line representing dopants fully ionized and a straight line with slope $-1/kT$ (for donor) or $1/kT$ (for acceptor) representing partially ionized dopants. The donor step

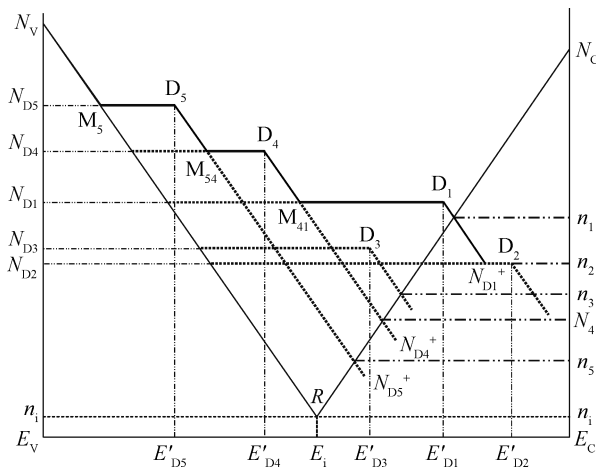


Fig. 2. Formation of the wrapping step function of multiple donor states and the mobile carrier holes, with the crossing points of D_i , the merging points M_5 (of hole $N_V R$ and 5th donor state $N_{D5} N_{D5}^+$), M_{34} (of 5th donor state $N_{D5} N_{D5}^+$ and 4th donor state $N_{D4} N_{D4}^+$), and M_{41} (of 4th donor state $N_{D4} N_{D4}^+$ and 1st donor state $N_{D1} N_{D1}^+$) to be rounded at $\pm 3kT$.

functions cross the line $N_C R$, which has a slope $1/kT$, and the acceptor step functions cross the line $N_V R$, which has a slope $-1/kT$. The cross point of $N_{D1} N_{D1}^+$ and $N_C R$ determines the electron doping level n if only one donor state D_i exists. Similar results are obtained for the acceptor states.

(3) The donor dopant state with the highest n ranks No. 1, and that with the second highest ranks No. 2, etc. The No. 1 donor is the dominant dopant, which determines the majority carrier electron density if there were only donors and no acceptors. We perform the same procedures for acceptor dopant states.

(4) The step functions of the donors form a positively charged hole-donor wrapping step function, which is shown in Fig. 2 for a semiconductor with 5 donor states with various ionization energies and concentrations. The ionization of, and contribution to, the electron density by D_3 , which is under the wrapping step function, and by D_2 , which is beyond the triangle $N_V R N_C$, are negligible. The doping level n is determined by the combination of its energy level E and density N . As shown in Fig. 2, the order of the energy levels of the dopants, the order of their concentrations, and the order of their doping levels are not the same. They must be obtained graphically or calculated numerically (not covered in this work). In a symmetrical way, we form the negatively charged electron-acceptor wrapping step function.

(5) We plot the two wrapping step functions of hole-donor (ionized) and of electron-acceptor (ionized) on the same semi logarithmic graph paper. We round up the representing points of the states, as well as the merging points between the states, and the merging point of the state and the carrier concentration straight line, as explained in Section 2. Facing each other, the two wrapping step functions cross each other, rendering the cross point with the Fermi level and the majority carrier density as its x - and y -coordinates. Note that the straight line $N_C R$ is a special case of the electron-acceptor wrapping step function when the acceptors are negligible, and the straight line $N_V R$ is

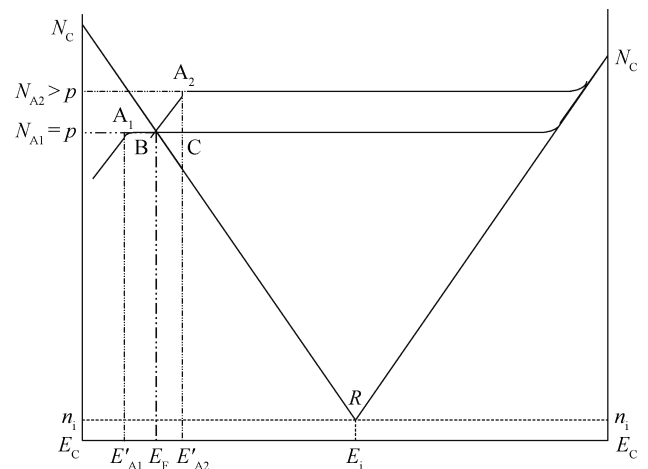


Fig. 3. Shallow acceptor state A_1 and non-shallow acceptor state A_2 ($N_V = 1.8 \times 10^{19} \text{ cm}^{-3}$).

a special case of hole-donor wrapping step function when the donors are negligible.

4. Examples of application of the graphical method

(1) Shallow and non-shallow dopants

As shown in Eq. (6) and Fig. 1, for a semiconductor with only one dopant state, the doping level is 50% of the dopant level when the ionization energy (strictly speaking, E'_D or E'_A , not E_D or E_A) is equal to the Fermi level. The closer the Fermi level to the band edge, the higher the carrier density. Based on this, the shallowness of a dopant level is defined by the difference between its ionization energy and the band edge^[2]. As shown in Fig. 1, however, $E_C - E'_{D1} < E_C - E'_{D2}$, yet state D_2 is fully ionized, and state D_1 is only partially ionized. Since the level or percentage of ionization of a state is referred to as the difference between the ionization energy and the Fermi level, we may want to consider an alternative definition of shallowness of the dopant states,

$$\left\{ \begin{array}{l} \text{Donor} \left\{ \begin{array}{l} \text{Shallow } E'_D - E_F > 3kT, > 95\% \text{ ionized,} \\ \text{Non-shallow } E_F - E'_D > 3kT, < 5\% \text{ ionized,} \end{array} \right. \\ \text{Acceptor} \left\{ \begin{array}{l} \text{Shallow } E_F - E'_A > 3kT, > 95\% \text{ ionized,} \\ \text{Non-shallow } E'_A - E_F > 3kT, < 5\% \text{ ionized.} \end{array} \right. \end{array} \right. \quad (9)$$

(2) Semiconductor with multiple dopants

It is generally agreed that the double acceptor Cd vacancy $V_{Cd} |^{0/-}$ ($E' = 0.15 \text{ eV}$, experimental value, quoted from Ref. [11]) and $V_{Cd} |^{-/-}$ (0.47 eV), the A-center $V_{Cd} - Cl_{Te} |^{0/-}$ (0.15 eV), and the impurity Cu substitution of Cd $Cu_{Cd} |^{0/-}$ (0.35 eV) are the three potentially responsible p-doping acceptors of the CdTe polycrystalline thin film in the commercially mostly successful photovoltaic technology CdS/CdTe solar cell^[9-12]. Multiple dopant states make it difficult to determine each state's concentration and its corresponding doping level, although they are the most fundamental parameters to be controlled in device processing. The graphical

Table 1. Possible concentrations of acceptor states A_1 and A_2 for p-CdTe thin film.

p (cm^{-3})	N_{A1} (cm^{-3}) only	N_{A2} (cm^{-3}) only	Possible combination of N_{A1} and N_{A2}
10^{14}	10^{14} , possible	4.1×10^{15} , possible	$0 < N_{A1} < 10^{14}$; $4.1 \times 10^{15} > N_{A2} > 0$
10^{15}	10^{15} , possible	4.1×10^{17} , impossible	$5 \times 10^{14} < N_{A1} < 10^{15}$; $10^{17} > N_{A2} > 0$

method presented in this work may resolve or alleviate the difficulty, leading to improvement of the material. Since the Cd vacancy acceptor and the A center have the same activation energy, they are treated as the same acceptor state A_1 , while the Cu substitute is A_2 . For example, by SIMS (secondary ion mass spectroscopy), we measure $N_{Cu} = 10^{17} \text{ cm}^{-3}$. Apparently, $N_{A2} < N_{Cu}$, since in addition to the substitute position, Cu can also be interstitial, or in the cluster or at grain boundaries^[10]. The relationship of the p-doping level, measured with 4- and Hall probe, and the probable dopant concentrations are obtained from the plot, as shown in Fig. 3 and Table 1.

(3) Graphical derivation of the equation of the doping level of non-shallow dopants

As shown in Fig. 3, the similarity of the triangles $N_V p B$ and $A_2 C B$ yields

$$\frac{\ln N_V - \ln p}{E_F - E_V} = \frac{\ln N_{A2} - \ln p}{E'_{A2} - E_F} = \frac{1}{kT}, \quad (10)$$

leading to the equation for calculating the non-shallow dopant's doping level as

$$p \approx \sqrt{N_V N_A} \exp\left(-\frac{E'_A - E_V}{2kT}\right) < N_A, \quad (11)$$

which is equivalent to the well-known analytically derived equation^[2],

$$p \approx \sqrt{\frac{N_V N_A}{g_A}} \exp\left(-\frac{E_A - E_V}{2kT}\right). \quad (12)$$

(4) Compensation of non-shallow dopant states

One may argue that the graphical method presented in this work is not necessary. Its merit is only convenience with visual insight. Indeed, all of the results of examples (1) to (3) may also be obtained from the numerical solution of Eq. (6). Now we study cases for which the intricacy of carrier compensation may not be clearly revealed without the graphical method.

The widely used equations for doping compensation (1) and (2) are only valid for shallow dopants, which are fully ionized with $N_D - N_D^+$ and $N_A - N_A^-$. For non-shallow dopants, such as the acceptor Cu_{Cd} , Cu substitute of Cd in p-CdTe thin film, compensated by the donor Cu_i , Cu interstitial, we resort to the graphical method to calculate the result of compensation, as shown in Fig. 4. Assume $N_V = 1.8 \times 10^{19} \text{ cm}^{-3}$, $E'_A - E_V = 0.35 \text{ eV}$, and $E'_C - E_D = 0.01 \text{ eV}$ (calculated, from Ref. [14]). Without donor compensation, we have p expressed by Eq. (11). With donor compensation, E_F is raised to E'_F and p is lowered to p' . From the similarity of the triangles as shown in the semi-logarithmic plot of Fig. 4, we have

$$\ln N_D - \ln p \approx \ln p - \ln p'. \quad (13)$$

Substituting Eq. (13) for Eq. (11), we have

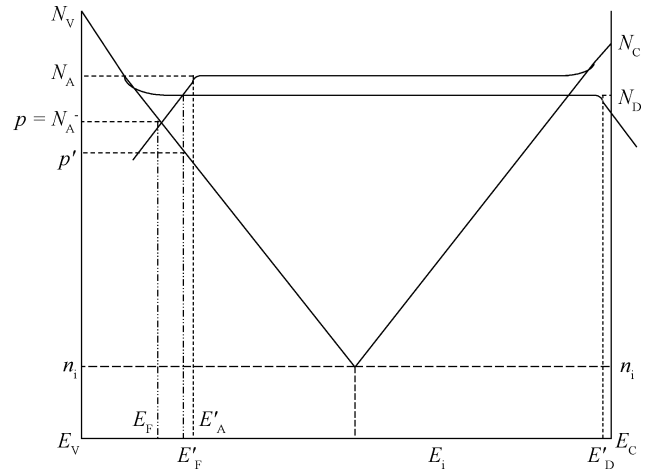


Fig. 4. Compensation of acceptor density N_A by donor density N_D , with $E_F \rightarrow E'_F$, and $p \rightarrow p'$.

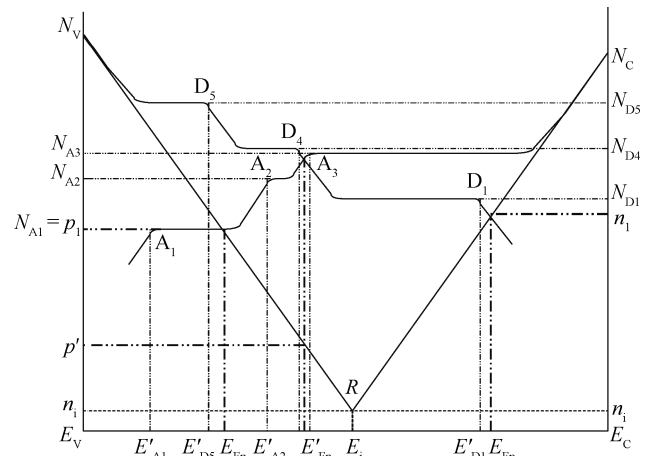


Fig. 5. Reversal of dopant and compensator; with $n_1 > p_1$ and $N_{D4} > N_{A3}$, yet the acceptors are dopants and the donors are compensators, rendering the holes as majority carriers.

$$p' \approx \frac{p^2}{N_D} = \frac{N_V N_A}{N_D} \exp\left(-\frac{E'_A - E_V}{kT}\right), \quad (14)$$

which shows, “surprisingly”, that the result of compensated hole density p' is not the widely quoted $N_A - N_D$, and it does not even depend on N_A so long as the ratio of N_A/N_D is kept a constant. This conclusion from the graphical method is only valid in a range where the compensation is significant—namely $1 > N_D/N_A > 0.1$ ^[17].

(5) Multiple acceptor states compensated by multiple donor states (or vice versa)

Figure 5 shows the result of the n-type semiconductor with multiple donor dopants as depicted by Fig. 2 compensated by multiple acceptor states. If there were only donors as the dom-

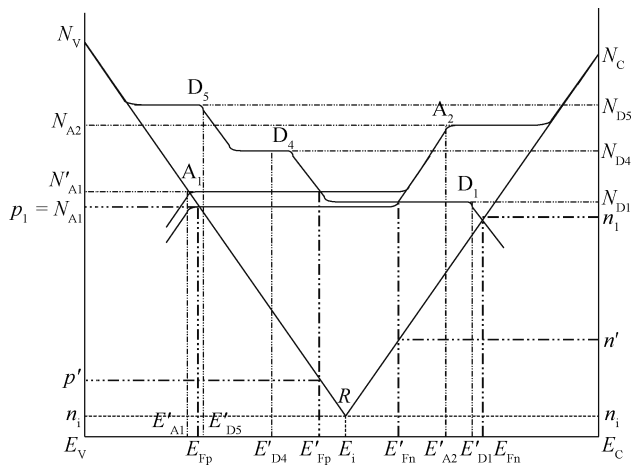


Fig. 6. Reversal of dopant and compensator; with $p_1 > n_1$ and $N_{A2} > N_{D1}$, yet the donors are dopants and the acceptors are compensators, rendering electrons as majority carriers.

inant dopant, the non-shallow donor state D_1 would render a doping level of n_1 for the material doped with multiple donor states. Similarly, if there were only acceptors as the dominant dopant, the shallow acceptor state A_1 would render a doping level of p_1 for the material doped with multiple acceptor states. When multiple donors and multiple acceptors coexist, we may think of the material as n-type compensated by acceptors, since $n_1 > p_1$, $N_{D5} < N_{A3}$; in terms of the dominant doping level and highest dopant density, the set of n-type donors seem to be the “stronger” dopants and the set of p-type acceptors seem to be the “weaker” compensators. However, as shown in the graph of Fig. 5, the role of dopants and compensators is reversed. The result of a donor compensated by an acceptor is a p-type semiconductor. Due to the donor compensation, the Fermi level of the p-type dopants moves up from E_{Fp} to E'_{Fp} , and the majority carrier hole density falls from p_1 to p' . A careful inspection of the graph reveals that it is not the sum of the acceptor states compensated by the sum of the donor states; it is actually only the acceptor state A_3 compensated by the donor state D_4 . In a one-to-one comparison of D_4 and A_3 , D_4 has a higher concentration but deeper energy level. It is the balance between the effect of concentration and the shallowness of the states that determines the result of compensation. Except for the pair of D_4 and A_3 , the other states and their doping levels have virtually no direct effect on the compensation; these states, however, may play the roles of electron and hole traps, resulting in the poor performance of many devices. Nevertheless, it is the complete set of multiple donors and multiple acceptors, with their wrapping step functions, which determine which donor–acceptor pair is the critical one. It is only through the graphical method that the critical role of A_3 and D_4 and the result of compensation are revealed clearly in the graph. If we put all of the concentrations and ionization energy levels of all of the states into Eq. (6), and use computer software to seek a numerical solution, we may obtain the Fermi level and the majority carrier density, but we will not know which states play the critical role in the compensation.

Figure 6 is another example of the reversal (often unexpected) of dopants and compensators. Although $p_1 > n_1$ (the

dominant acceptor state A_1 in an acceptor-only material has a higher doping level than the dominant donor state D_1 in a donor-only material), and $N_{A2} > N_{D1}$ (the critical acceptor state has a higher concentration than the critical donor state), as shown by our graph, the donors are dopants and the acceptors are compensators for the system, rendering electrons as the majority carriers. The Fermi level E_{Fn} without acceptors' compensation falls to E'_{Fn} after compensation, while the electron density without compensation n_1 falls to n' . Moreover, Figure 6 shows that a small increase in the concentration of the acceptor state A_1 from N_{A1} to N'_{A1} will change “unexpectedly” the semiconductor from n-type to p-type, with Fermi level E'_{Fp} and majority carrier density p' . This example shows how uncertain and vulnerable the multiply doped semiconductor may be. Sudden, unexpected change in the material may occur due to some inadvertent or even trivial variation in the processing condition of the material. Following the guidance of the graphical method, which is impossible to get from the PC based numerical solution, we may be able to pay special attention to some specific procedures to make the semiconductor with the desired properties. The processing of CdTe thin film is such an example, which involves the control of all of the potentially responsible non-shallow dopants and compensators.

5. Conclusion and discussion

In conclusion:

- (1) We have introduced in detail a generic and simple-to-follow approximate graphic plotting method to represent and solve the equation of LCN on semi-logarithmic graph paper.
- (2) By using the graphical method, we gain a visual insight into the doping mechanism of semiconductor materials, based on which we introduce an alternative definition of the shallowness of a dopant state by the level (percentage) of its ionization.
- (3) By using the graphical method, we may be able to derive the known equations, such as the non-shallow dopant's partial ionization, in a simpler and visually insightful way.
- (4) By using the graphical method, we may be able to derive some new equations, such as the compensation of the non-shallow dopants.
- (5) By using the graphical method, we not only solve for the Fermi level and majority carrier density but we may also solve other unknowns, such as the dopant concentration and the combination of the multiple dopant concentrations if the Fermi level is known.
- (6) When using the graphical method, we not only obtain the Fermi level (with it the majority carrier density) but we may also gain an insight into the material that the numerical method fails to offer. For example, among the multiple donor states and acceptor states, which pair of donor and acceptor plays the critical role in the determination of the Fermi level, and which state (or states) are crucially sensitive, the small variation of which may render the semiconductor with surprisingly different properties.
- (7) The concentrations and activation energy levels are inputs to the graphic presentation of the LCN equation. We are working to acquire these parameters more accurately, especially for CdTe, to make the graphical method more useful.

Acknowledgement

The author acknowledges helpful discussions with, and suggestions from, Professor H. Kroemer of UC, Santa Barbara, T. Gessert, S. Wei, Q. Wang, and D. Friedman of NREL, G. Wang, J. S. Liu, and Z. Zheng of BUAA, China, and G. Georgiou, and Z. Cheng of NJIT.

References

- [1] Sze S. Physics of semiconductor devices. 2nd ed. New York: Wiley, 1981
- [2] Blood P, Orton J W. The electrical characterization of semiconductors: majority carriers and electron states. Academic Press, 1992
- [3] Orton J W, Blood P. The electrical characterization of semiconductors: measurement of minority carrier properties. Academic Press, 1990
- [4] Look D C. Semi-conductors and semi-metals. Willardson R K, Beer A C, ed. New York: Academic Press, 1983
- [5] Harafuji T, Kawamura J. Molecular dynamics simulation for evaluating melting point of wurtzite-type GaN crystal. Appl Phys, 2005, 96: 2501
- [6] Akasaki I, Amano H. Crystal growth and conductivity control of group III nitride semiconductors and their application to short wavelength light emitters. Jpn J Appl Phys, 1997, 36: 5393
- [7] Minami T. Transparent conducting oxide semiconductors for transparent electrodes. Semicond Sci Technol, 2005, 20: S35
- [8] Mamazza R Jr, Morel D L, Ferekides C S. Transparent conducting oxide thin films of Cd_2SnO_4 prepared by RF magnetron co-sputtering of the constituent binary oxides. Thin Solid Films, 2005, 484(1/2): 26
- [9] Wu X. High-efficiency polycrystalline thin-film solar cells. Solar Energy, 2004, 77: 803
- [10] Gessert T A, Metzger W K, Dippo P, et al. Dependence of carrier lifetime on copper-contacting temperature and ZnTe:Cu thickness in CdS/CdTe thin film solar cells. Thin Solid Films, 2009, 517: 2370
- [11] Seymour F. Studies of electronic states controlling the performance of CdTe solar cells. PhD (Materials Science) Thesis, Colorado School of Mines, 2005: 35
- [12] Attygalle M L C. Theoretical modeling of polycrystalline thin-film photovoltaics. PhD Dissertation of Physics, University of Toledo, 2008
- [13] Kittel C, Kroemer H. Thermal physics. 2nd ed. New York: Freeman, 1980
- [14] Wei S H, Zhang S B. Chemical trends of defect formation and doping limit in II-VI semiconductors: the case of CdTe. Phys Rev B, 2002, 66: 15521